The Canadian Mineralogist
Vol. 35, pp. 1515-1522 (1997)

REFINEMENT OF THE CRYSTAL STRUCTURE OF BURANGAITE

JULIE B. SELWAY[1], MARK A. COOPER AND FRANK C. HAWTHORNE

Department of Geological Sciences, University of Manitoba, Winnipeg, Manitoba R3T 2N2

ABSTRACT

The crystal structure of burangaite, $Na_{0.96}(Fe^{2+}_{0.55}Mg_{0.33}Fe^{3+}_{0.10}Mn_{0.02})_{\Sigma 1.00}Al_{4.89}(PO_4)_{4.06}(OH)_6(H_2O)_2$, *a* 25.099(2), *b* 5.0491(7), *c* 13.438(1) Å, ß 110.88(1)°, *V* = 1591.1(3) Å^3, *C2/c*, *Z* = 4, has been refined to an *R* index of 2.8% for 2004 observed reflections measured with Mo*K*α X-radiation. Burangaite is isostructural with dufrénite, considered by Moore (1970) to have a composition between $Ca_{0.5}Fe^{2+}Fe^{3+}_5(PO_4)_4(OH)_6(H_2O)_2$ and $\square Fe^{3+}Fe^{3+}_5(PO_4)_4(OH)_6(H_2O)_2$. The fundamental building block (FBB) of the structure of burangaite is a face-sharing triplet of octahedra [$Al\phi_6 - Fe\phi_6 - Al\phi_6$] corner-linked to two $Al\phi_6$ octahedra and two PO_4 tetrahedra. The FBB is polymerized parallel to the **c** axis to form dense slabs in the {100} plane. Alternating $Al\phi_6$ octahedra and $Na\phi_8$ polyhedra form a chain parallel to the **c** axis, and the dense slab and chain alternate along the **a** axis.

Keywords: burangaite, single-crystal structure refinement, dufrénite, granitic pegmatite, Buranga, Rwanda.

SOMMAIRE

Nous avons affiné la structure cristalline de la burangaïte, $Na_{0.96}Fe^{2+}_{0.55}Mg_{0.33}Fe^{3+}_{0.10}Mn_{0.02})_{\Sigma 1.00}Al_{4.89}(PO_4)_{4.06}(OH)_6(H_2O)_2$, *a* 25.099(2), *b* 5.0491(7), *c* 13.438(1) Å, ß 110.88(1)°, *V* = 1591.1(3) Å^3, *C2/c*, *Z* = 4, jusqu'à un résidu *R* de 2.8% en utilisant 2004 réflexions observées, mesurées avec rayonnement Mo*K*α. La burangaïte est isostructurale avec la dufrénite qui, selon Moore (1970), a une composition entre $Ca_{0.5}Fe^{2+}Fe^{3+}_5(PO_4)_4(OH)_6(H_2O)_2$ et $\square Fe^{3+}Fe^{3+}_5(PO_4)_4(OH)_6(H_2O)_2$. Le bloc structural fondamental de la structure est un trio d'octaèdres à faces partagées, [$Al\phi_6 - Fe\phi_6 - Al\phi_6$], dont les coins sont liés à deux octaèdres $Al\phi_6$ et deux tétraèdres PO_4. Le bloc fondamental est polymérisé en panneaux denses parallèles à l'axe **c**, dans le plan {100}. Des octaèdres $Al\phi_6$ et des polyèdres $Na\phi_8$ en alternance forment des chaînes parallèles à l'axe **c**; les panneaux denses et les chaînes alternent le long de l'axe **a**.

(Traduit par la Rédaction)

Mots-clés: burangaïte, affinement de la structure, cristal unique, dufrénite, pegmatite granitique, Buranga, Rwanda.

INTRODUCTION

Burangaite, ideally $(Na,Ca)(Fe^{2+},Mg)Al_5(PO_4)_4(OH,O)_6(H_2O)_2$, was first described by von Knorring *et al.* (1977) from the Buranga granitic pegmatite, Rwanda. It occurs as long prismatic blue crystals associated with bertossaite, trolleite, scorzalite (which it replaces), apatite, bjarebyite and wardite (von Knorring *et al.* 1977). Recently, a Mg-analogue of burangaite has been described from one of the largest producers of gold in North America, the Gold Quarry mine, Nevada (Jensen *et al.* 1995), a hydrothermal gold deposit with relatively abundant phosphate minerals. The burangaite analogue occurs in rare vugs in partly silicified pyrite-rich alunite-bearing barite breccia. It forms pale-green radiating groups and hemispheres of prismatic crystals associated with englishite, crandallite, carbonate-fluorapatite and variscite.

EXPERIMENTAL

The material used in this work is from the type locality, the Buranga pegmatite, and was kindly donated by Forrest Cureton. A single crystal was mounted on a Nicolet *R*3*m* automated four-circle diffractometer. Thirteen reflections over the range $8 < 2\theta < 27°$ were centered using graphite-monochromated Mo*K*α X-radiation. The cell dimensions (Table 1) were derived from the setting angles of these reflections by least-squares refinement. Data were collected using the θ–2θ scan method, with a scan range of 2.2°, and a variable scan-rate inversely proportional to the peak intensity, with maximum and minimum scan-rates of 29.3° and 3.9°/min, respectively. A total of 2628 reflections were measured over the range $4° \le 2\theta \le 60°$, with ranges in indices $0 \le h \le 36$, $0 \le k \le 8$, $-19 \le l \le 19$. One standard

[1] *E-mail address*: umselway@cc.umanitoba.ca

reflection was measured every eighty reflections; there was no significant change in its intensity during data collection. A psi-scan absorption-correction was applied, with the crystal modeled as an ellipsoid. The data were merged and corrected for Lorentz and polarization effects, and background.

TABLE 1. MISCELLANEOUS INFORMATION FOR BURANGAITE

a (Å)	25.099(2)	crystal size (mm)	0.21 x 0.13 x 0.15
b	5.0491(7)	Radiation	MoKα
c	13.438(1)	Total no. of I	2628
β	110.88(1)	No. of $\|F\|$	2331
V (Å^3)	1591.1(3)	No. of $\|F\| > 5\sigma$	2004
Sp. Gr.	$C2/c$	R(azimuthal) %	2.2 → 1.2
μ (cm^{-1})	15.9	R(obs) %	2.8
D_{calc} (g/cm^3)	3.00	wR(obs) %	3.1

cell content : $4[Na(Fe,Mg)Al_3(PO_4)_4(OH)_6(H_2O)_2]$

$R = \Sigma(|F_o| - |F_c|)/\Sigma|F_o|$

$wR = [\Sigma w(|F_o| - |F_c|)^2/\Sigma F^2_o]^{1/2}$, $w = 1$

Structure Refinement

Scattering curves for neutral atoms, together with anomalous dispersion corrections, were taken from Cromer & Mann (1968) and Cromer & Liberman (1970), respectively. R indices are of the form given in Table 1 and are expressed as percentages. The Siemens SHELXTL PLUS (PC version) system of programs was used throughout this study. Refinement was initiated using the dufrénite model of Moore (1970), and converged to an R index of 3.1%. A three-dimensional difference-Fourier map was calculated at this stage of the refinement, and five hydrogen atoms were found, all at the 8f position. The "soft" constraint that the donor–hydrogen distance should be ~0.98 Å was imposed by adding extra weighted observational equations to the least-squares matrix. Only the donor–hydrogen distance is constrained, and the hydrogen position is free to seek its optimum position around the donor atom. Refinement of all parameters gave a final R index of 2.8% and a wR index of 3.1%. Final

TABLE 2. FINAL POSITIONAL AND DISPLACEMENT PARAMETERS FOR BURANGAITE

Site	x	y	z	$*U_{eq}$	U_{11}	U_{22}	U_{33}	U_{23}	U_{13}	U_{12}
Na	0	-0.1475(3)	¼	139(5)	110(8)	190(8)	122(8)	0	46(6)	0
Al(1)	0	0	0	61(3)	52(5)	69(5)	63(5)	-4(4)	21(4)	1(4)
Fe(2)	¼	¼	0	63(2)	53(3)	68(3)	59(3)	-3(2)	8(2)	-46(2)
Al(3)	0.15172(3)	-0.0184(2)	0.10937(5)	51(2)	51(3)	57(4)	47(3)	-4(2)	19(2)	-3(3)
Al(4)	0.14090(3)	-0.2243(1)	0.35101(5)	46(2)	51(3)	45(3)	43(3)	2(3)	18(2)	8(3)
P(1)	0.21594(2)	0.2660(1)	0.32744(4)	45(2)	46(2)	43(3)	45(2)	-1(2)	17(2)	-1(2)
P(2)	0.08058(2)	0.2752(1)	0.39430(5)	49(2)	49(2)	47(3)	55(2)	2(2)	22(2)	0(2)
O(1)	0.09188(7)	0.0558(4)	0.3256(1)	77(5)	84(7)	63(8)	82(7)	-9(6)	27(6)	18(6)
O(2)	0.07990(7)	0.5443(4)	0.3412(1)	70(5)	75(7)	56(7)	81(7)	18(6)	29(6)	-3(6)
O(3)	0.02109(7)	0.2212(4)	0.4013(1)	84(5)	57(7)	96(8)	109(7)	21(6)	45(6)	-4(6)
O(4)	0.12559(7)	0.2796(4)	0.5061(1)	76(5)	89(7)	70(7)	56(7)	7(6)	12(6)	-12(6)
O(5)	0.16661(7)	0.2148(4)	0.0085(1)	76(5)	85(7)	83(8)	73(7)	-2(6)	45(6)	3(6)
O(6)	0.20824(7)	0.0037(4)	0.3798(1)	75(5)	74(7)	67(8)	77(7)	22(6)	20(6)	-2(6)
O(7)	0.19596(7)	-0.5027(4)	0.3816(1)	73(5)	78(7)	63(7)	77(7)	-18(6)	28(6)	10(6)
O(8)	0.12955(7)	-0.2502(4)	0.2046(1)	69(5)	79(7)	71(8)	62(7)	5(6)	33(6)	1(6)
O(9)	0.17616(7)	0.2552(4)	0.2105(1)	77(5)	87(7)	76(8)	58(7)	-5(6)	13(6)	3(6)
O(10)	0.22232(7)	-0.1896(4)	0.1574(1)	96(5)	65(7)	103(8)	125(8)	19(7)	42(6)	15(6)
O(11)	0.07453(7)	0.1270(4)	0.0660(1)	82(5)	55(7)	77(8)	106(8)	-12(6)	19(6)	-2(6)
O(12)	0.02132(7)	-0.2822(4)	0.1022(1)	96(5)	82(8)	100(8)	104(8)	20(7)	30(6)	-3(7)
H(5)	0.153(2)	0.392(4)	0.018(4)	500						
H(8)	0.145(2)	-0.423(4)	0.195(4)	500						
H(11)	0.079(2)	0.231(9)	0.130(2)	500						
H(12A)	0.004(2)	-0.457(4)	0.098(4)	500						
H(12B)	0.0630(2)	-0.29(1)	0.134(3)	500						

*U_{ij} values have been multiplied by 10^4.

TABLE 3. SELECTED INTERATOMIC DISTANCES (Å) AND ANGLES (°) IN BURANGAITE

P(1)-O(6)	1.544(2)		*Fe*(2)-O(5),f	2.144(2)	x2
P(1)-O(7)a	1.551(2)		*Fe*(2)-O(6)b,g	2.035(2)	x2
P(1)-O(9)	1.533(2)		*Fe*(2)-O(7)h,g	2.112(2)	x2
P(1)-O(10)b	1.506(2)		<*Fe*(2)-O>	2.097	
<*P*(1)-O>	1.534				
P(2)-O(1)	1.531(2)		*Na*-O(1),c	2.395(2)	x2
P(2)-O(2)	1.532(2)		*Na*-O(2)i,k	2.489(2)	x2
P(2)-O(3)	1.553(2)		*Na*-O(3),c	2.667(2)	x2
P(2)-O(4)	1.525(2)		*Na*-O(12),c	2.334(2)	x2
<*P*(2)-O>	1.535		<*Na*-O>	2.471	
Al(1)-O(3)c,d	1.946(2)	x2	H(5)-O(5)	0.98(3)	
Al(1)-O(11),e	1.875(2)	x2	H(5)···O(4)l	1.78(3)	
Al(1)-O(12),e	1.918(2)	x2	O(5)-H(5)···O(4)l	168(5)	
<*Al*(1)-O>	1.913				
Al(3)-O(4)g	1.856(2)		H(8)-O(8)	0.98(3)	
Al(3)-O(5)	1.929(2)		H(8)···O(9)i	1.79(3)	
Al(3)-O(8)	1.956(2)		O(8)-H(8)···O(9)i	166(4)	
Al(3)-O(9)	1.881(2)				
Al(3)-O(10)	1.868(2)		H(11)-O(11)	0.98(4)	
Al(3)-O(11)	1.956(2)		H(11)···O(9)	2.29(5)	
<*Al*(3)-O>	1.908		O(11)-H(11)···O(9)	103(3)	
Al(4)-O(1)	1.825(2)		H(12A)-O(12)	0.98(3)	
Al(4)-O(2)i	1.893(2)		H(12A)···O(3)m	1.74(3)	
Al(4)-O(5)j	1.981(2)		O(12)-H(12A)···O(3)m	174(4)	
Al(4)-O(6)	1.966(2)		H(12B)-O(12)	0.980(6)	
Al(4)-O(7)	1.911(2)		H(12B)···O(8)	1.61(1)	
Al(4)-O(8)	1.889(2)		O(12)-H(12B)···O(8)	167(5)	
<*Al*(4)-O>	1.911		H(12A)···H(12B)	1.63(5)	
			H(12A)-O(12)-H(12B)	112(4)	

a: x, 1+y, z; b: ½-x, ½+y, ½-z; c: -x, y, ½-z; d: x, -y, -½+z; e: -x, -y, -z; f: ½-x, ½-y, -z; g: x, -y, z-½; h: ½-x, y+½, ½-z; i: x, y-1, z; j: x, -y, z+½; k: -x, y-1, ½-z; l: x, 1-y, z-½; m: -x, y-1, ½-z

positional and displacement parameters are given in Table 2, selected interatomic distances and angles in Table 3, and a bond-valence analysis in Table 4. The H bond-valence is assigned to minimize deviations from the bond-valence rule. Observed and calculated structure-factors are available from the Depository of Unpublished Data, CISTI, National Research Council, Ottawa, Ontario K1A 0S2.

Chemical Composition

The crystal used in the collection of the X-ray intensity data was subsequently mounted in epoxy, ground, polished and analyzed by electron microprobe using a CAMECA SX–50 according to the procedure of Hawthorne *et al.* (1993). Crystals were analyzed using $K\alpha$ lines from the following standards: albite (Na), kyanite (Al), apatite (P, Ca), olivine (Mg), fluor-riebeckite (F), fayalite (Fe), spessartine (Mn), orthoclase (K) and diopside (Si). The results (mean of 11 points) are given in Table 5. The formula, based on 24 anions with 6 (OH) groups and 2 (H_2O) groups, is $Na_{0.96}(Fe^{2+}_{0.55}Mg_{0.33}Fe^{3+}_{0.10}Mn_{0.02})_{\Sigma 1.00}Al_{4.89}(PO_4)_{4.06}(OH)_6(H_2O)_2$. The strong pleochroism and presence of Fe^{3+} detected by wet-chemical analysis by von Knorring *et al.* (1977) are significant evidence for the presence of Fe^{3+}. The site population for *Fe*(2) is 0.65 Fe* + 0.33 Mg + 0.02 Mn^{2+}. Assuming that all Fe* is in the ferrous state gives an aggregate cation radius of 0.761 Å and a predicted <*Fe*(2)–O> distance of 0.761 + 1.360 = 2.114 Å. The observed <*Fe*(2)–O> distance of 2.097 Å is significantly shorter than this distance predicted for all Fe^{2+} at *Fe*(2). Adjusting the Fe^{2+} and Fe^{3+} contents of *Fe*(2) to produce the required predicted distance of 2.097 Å gives a site population of 0.55 Fe^{2+} + 0.10 Fe^{3+} + 0.33

TABLE 4. BOND-VALENCE* TABLE FOR BURANGAITE

	Na	*Al*(1)	*Fe*(2)	*Al*(3)	*Al*(4)	*P*(1)	*P*(2)	H(5)	H(8)	H(11)	H(12A)	H(12B)	Σ
O(1)	0.19$^{\times 2}\downarrow$				0.62		1.28						2.09
O(2)	0.15$^{\times 2}\downarrow$				0.52		1.28						1.95
O(3)	0.10$^{\times 2}\downarrow$	0.45$^{\times 2}\downarrow$					1.20				0.30		2.05
O(4)				0.57			1.30	0.20					2.07
O(5)			0.33$^{\times 2}\downarrow$	0.47	0.41			0.80					2.01
O(6)			0.43$^{\times 2}\downarrow$		0.43	1.24							2.10
O(7)			0.35$^{\times 2}\downarrow$		0.50	1.21							2.06
O(8)				0.44	0.52				0.80			0.30	2.16
O(9)				0.54		1.27			0.20	0.05			2.06
O(10)				0.55		1.37							1.93
O(11)		0.54$^{\times 2}\downarrow$		0.44						0.95			1.93
O(12)	0.22$^{\times 2}\downarrow$	0.49$^{\times 2}\downarrow$									0.70	0.70	2.11
Σ	1.32	2.96	2.22	3.01	3.00	5.09	5.06	1.00	1.00	1.00	1.00	1.00	

* calculated from the curves of Brown (1981)

TABLE 5. CHEMICAL COMPOSITION* AND UNIT FORMULA OF BURANGAITE

P_2O_5	39.38	wt%	P	4.06
Al_2O_3	34.11		Al	4.89
Fe_2O_3++	1.15			
MgO	1.82		Fe^{3+}	0.10
MnO	0.16		Fe^{2+}	0.55
FeO	5.36		Mg	0.33
Na_2O	4.05		Mn	0.02
H_2O**	12.32		Σ	1.00
sum	98.35			
			Na	0.96
			OH	6.00
			H_2O	2.00

*Si, Ca, K, F were not detected; ++ calculated based on <*Fe*(2)-O>; **calculated from stoichiometry; analysis is the mean of 11 values.

Cation Coordination

Phosphorus occurs at two symmetrically distinct sites, *P*(1) and *P*(2), each coordinated by four O anions in a tetrahedral arrangement. The mean bond-lengths <*P*(1)–O> = 1.534 Å and <*P*(2)–O> = 1.535 Å are typical for P in tetrahedral coordination by O anions (Table 3) (Baur 1974). Aluminum occurs at three symmetrically distinct sites, *Al*(1), *Al*(3) and *Al*(4), each of which is coordinated by six anions in an octahedral arrangement. The *Al*(1) site is coordinated by two O anions, two (OH) groups and two (H_2O) groups, with <*Al*(1)–O> = 1.913 Å. The *Al*(3) site is coordinated by three O anions and three (OH) groups, with <*Al*(3)–O> = 1.908 Å. The *Al*(4) site is coordinated by four O anions and two (OH) groups, with <*Al*(4)–O> = 1.911 Å. The scattering at the *Al* sites is compatible with complete occupancy of these sites by Al, a conclusion in accord with the <*Al*–ϕ> bond-lengths (ϕ: unspecified anionic species).

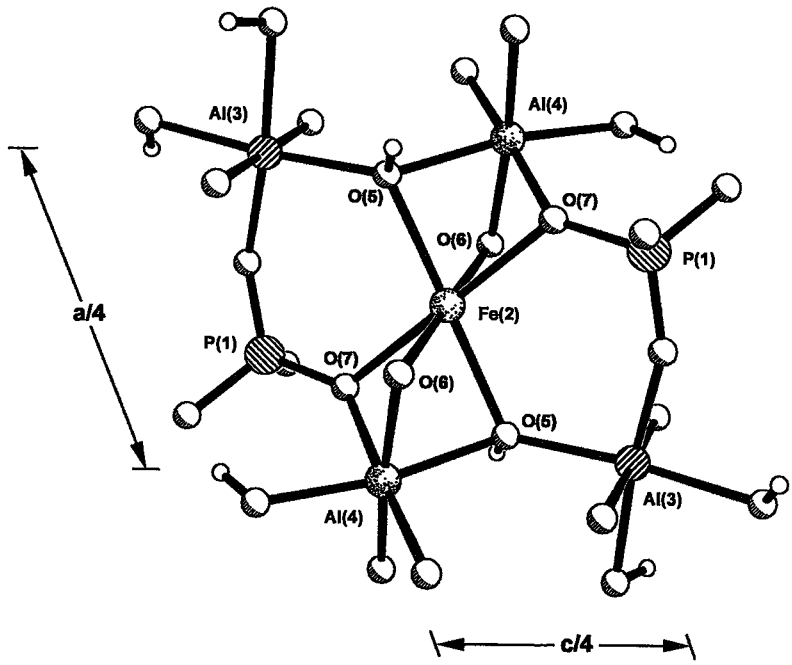

FIG. 1. The fundamental building block of the burangaite structure projected onto (010).

Mg + 0.02 Mn^{2+}. Von Knorring *et al.* (1977) reported 0.25 *apfu* (atoms per formula unit) Ca in burangaite from Rwanda (calculated on the basis of 24 anions), but we did not detect Ca during electron-microprobe analysis.

The *Fe*(2) site is coordinated by four O anions and two (OH) groups in an octahedral arrangement. The refined site-scattering at the *Fe*(2) site is 20.9(3) *epfu* (electrons per formula unit), within 2σ of the calculated scattering of 21.4 *epfu* assigned from the unit formula

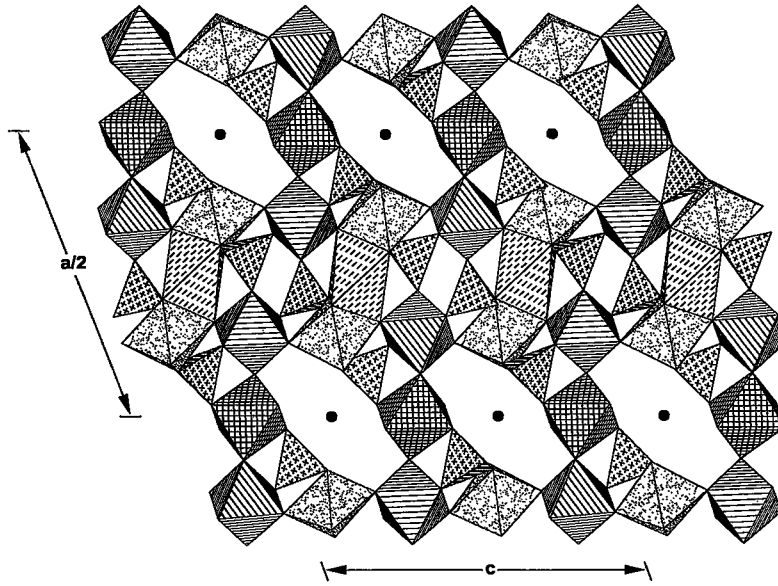

FIG. 2. The burangaite structure projected onto (010); PO_4 tetrahedra have crossed shading, $Al(1)\phi_6$ octahedra have hatched shading, $Al(3)\phi_6$ octahedra have parallel-line shading, $Al(4)\phi_6$ octahedra have random-dot shading, $Fe(2)\phi_6$ octahedra have dashed shading, and *Na* cations have solid shading.

(Table 5); thus the *Fe*(2) site is occupied by Fe^{2+}, Mg, Fe^{3+} and Mn^{2+}. The *Na* site is coordinated by six O anions and two (H_2O) groups to form a cubic antiprism with <*Na*–O> = 2.471 Å.

TOPOLOGY OF THE STRUCTURE

The fundamental building block (FBB) in burangaite contains one $Fe(2)\phi_6$ octahedron, two $Al(4)\phi_6$ octahedra, two $Al(3)\phi_6$ octahedra, and two $P(1)O_4$ tetrahedra (Fig. 1). The $Fe(2)\phi_6$ octahedron shares faces with the two $Al(4)\phi_6$ octahedra through the O(5), O(6) and O(7) anions to form a face-sharing triplet of octahedra of the form $[M_3\phi_{12}]$, where *M* is any octahedrally coordinated cation. This face-sharing triplet of octahedra that forms the core of the FBB was named the *h*-cluster by Moore (1970). The *h*-cluster is corner-linked to two $Al(3)\phi_6$ octahedra and two $P(1)O_4$ tetrahedra to produce a cluster of the general form $[M_5(TO_4)_2\phi_{18}]$. The FBB is polymerized along the **c** axis to form a dense slab by corner-sharing of $Al(3)\phi_6$ octahedra of one FBB to $Al(4)\phi_6$ octahedra and $P(1)O_4$ tetrahedra of another FBB (Fig. 2). This slab is oriented parallel to {100}, and much weaker linkage between adjacent slabs produces perfect {100} cleavage in burangaite.

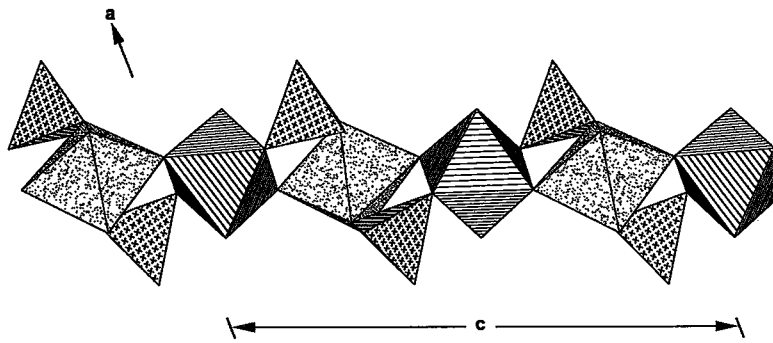

FIG. 3. Chain of alterating $Al(3)\phi_6$ octahedra and $Al(4)\phi_6$ octahedra parallel to **c** axis; legend as in Fig. 2.

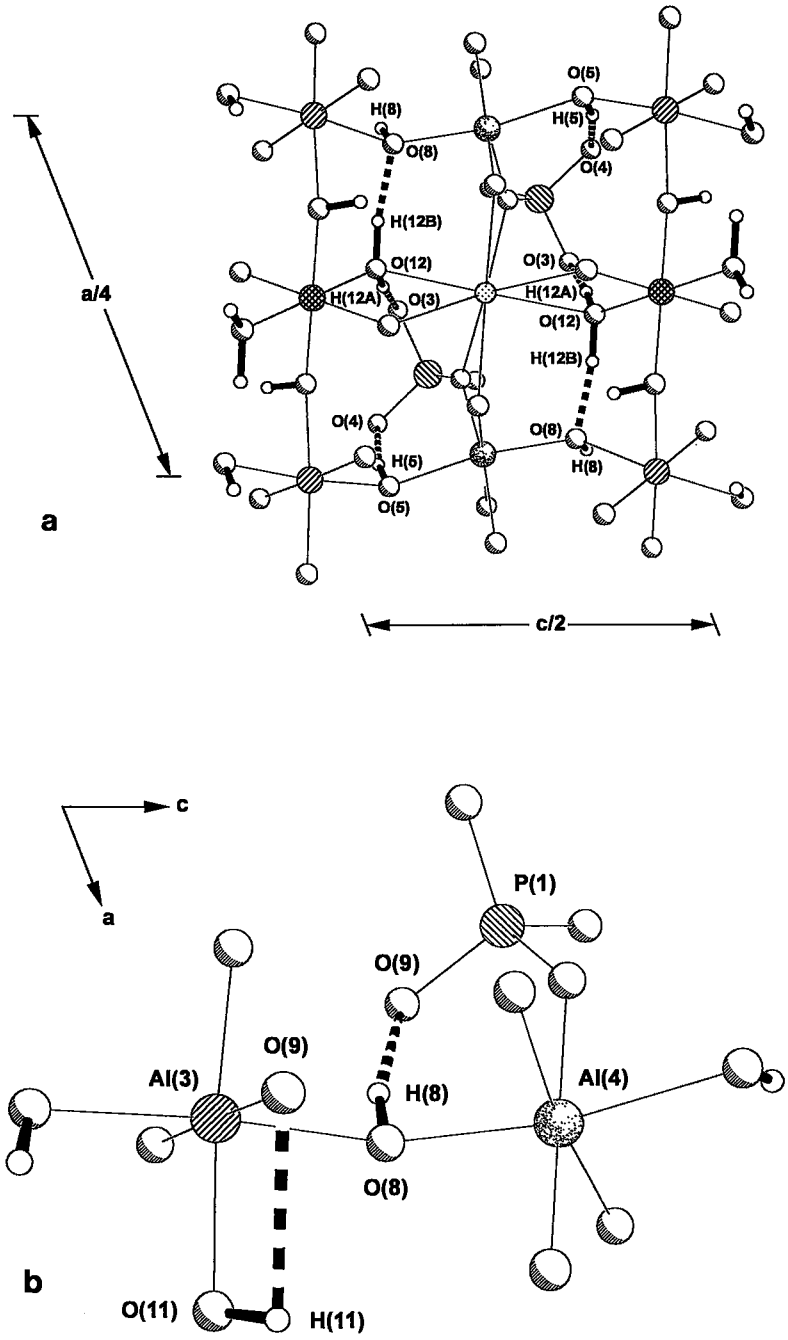

FIG. 4. Hydrogen bond in the structure of burangaite projected onto (010): (a) hydrogen bonding for H(5), H(12A) and H(12B), and (b) hydrogen bonding for H(8) and H(11). D–H and H...A bonds (D: donor, A: acceptor) are given as heavy full and broken lines, respectively. *Al*(3) cations have bottom left to top right parallel-line shading, *Al*(4) cations have heavy random-dot shading, *P*(1) and *P*(2) cations have bottom right to top left parallel-line shading, *Al*(1) cations have hatched shading, and *Na* cation has regular-dot shading.

Alternatively, one can view these slabs as consisting of decorated $[M\phi_5]$ chains, consisting of alternating $Al(3)\phi_6$ and $Al(4)\phi_6$ octahedra, parallel to **c** (Fig. 3). These $[M\phi_5]$ chains are cross-linked *via* face-sharing between $Al(4)\phi_6$ octahedra of the chain and $Fe\phi_6$ octahedra, and *via* corner-sharing between octahedra of the chain and $P(1)O_4$ and $P(2)O_4$ tetrahedra. This decorated chain has the general form $[M(TO_4)\phi_3]$.

Hydrogen Bonding

There are five symmetrically distinct H sites, H(5), H(8), H(11), H(12A) and H(12B), labeled after the O atoms with which they form strong donor bonds. The H atoms and their associated O anions form three symmetrically distinct (OH) groups and one (H_2O) group. H(5) forms a hydrogen bond with O(4), and H(8) forms a hydrogen bond with O(9) on a lower structural level (Figs. 4a, b). The situation for H(11) is less clear. Possibly H(11) forms a hydrogen bond with O(9), but it must be quite weak, as the H...O distance is relatively long (2.29 Å) and the O(11)–H(11)...O(9) angle is very small (103°) (Table 3). The O(12) forms donor bonds with H(12A) and H(12B); H(12A) forms a strong hydrogen bond with O(3), and H(12B) forms a hydrogen bond with O(8) (Fig. 4a).

Comparison with Other Minerals

Burangaite, whose end-member composition is $NaFe^{2+}Al_5(PO_4)_4(OH)_6(H_2O)_2$, is isostructural with natrodufrénite and dufrénite (Moore 1970, Fontan *et al.* 1982). Natrodufrénite, $(Na,\square)(Fe^{3+},Fe^{2+})(Fe^{3+},Al)_5(PO_4)_4(OH)_6(H_2O)_2$, is the Fe^{3+} equivalent of burangaite. It is clear from the cell dimensions reported by Fontan *et al.* (1982) that these two minerals are isostructural. The structural model refined here for burangaite is that of Moore (1970, p. 147) for dufrénite. Moore (1970) gave the formula of dufrénite as $Ca_{0.5}Fe^{2+}Fe^{3+}_5(PO_4)_4(OH)_6(H_2O)_2$. However, both Moore (1984) and Nriagu (1984) gave the formula of dufrénite as $CaFe^{3+}_6(PO_4)_4(OH)_6(H_2O)_2$, which is not neutral (it has a charge of 2+); this is presumably a misquote of Moore (1970), but has propagated through the literature. Van der Westhuizen *et al.* (1990) reported electron-microprobe compositions for dufrénite from Kangnas farm, South Africa, and compared these with the results of Frondel (1949). They stated that Ca substitution is minor even in samples reported as pure dufrénite. However, some of the dufrénite compositions they reported (*e.g.*, with 8.7 Fe^{3+} and 1.95 P *apfu*) are completely incompatible with the structure of Moore (1970) (*cf.* Fontan & Fransolet 1992). The current situation with regard to dufrénite is rather confused; an extensive study is planned to try to resolve these problems.

Acknowledgements

We thank Forrest Cureton for generously supplying the material used here, and John Hughes and Don Peacor for their comments on the manuscript. This work was supported by a University of Manitoba Fellowship to JBS, and by Natural Sciences and Engineering Research Council of Canada Operating, Infrastructure and Major Equipment Grants to FCH.

References

Baur, W.H. (1974): The geometry of polyhedral distortions. Predictive relationships for the phosphate group. *Acta Crystallogr.* **B30**, 1195-1215.

Brown, I.D. (1981): The bond valence method: an empirical approach to chemical structure and bonding. *In* Structure and Bonding in Crystals **II** (M. O'Keeffe & A. Navrotsky, eds.). Academic Press, New York, N.Y. (1-30).

Cromer, D.T. & Liberman, D. (1970): Relativistic calculation of anomalous scattering factors for X-rays. *J. Chem. Phys.* **53**, 1891-1898.

_____ & Mann, J.B. (1968): X-ray scattering factors computed from numerical Hartree–Fock wave functions. *Acta Crystallogr.* **A24**, 321-324.

Fontan, F. & Fransolet, A.-M. (1992): Dufrenite in iron-formation on the Kangnas farm, Aggeneys district, Bushmanland, South Africa: a comment. *Mineral. Mag.* **56**, 426-427.

_____, Pillard, F. & Permingeat, F. (1982): La natrodufrénite $(Na,\square)(Fe^{+++},Fe^{++})(Fe^{+++},Al)_5(PO_4)_4(OH)_6.2H_2O$, une nouvelle espèce minérale du groupe de la dufrénite. *Bull. Minéral.* **105**, 321-326.

Frondel, C. (1949): The dufrenite problem. *Am. Mineral.* **34**, 513-540.

Hawthorne, F.C., Ungaretti, L., Oberti, R., Bottazzi, P. & Czamanske, G.K. (1993): Li: an important component in igneous alkali amphiboles. *Am. Mineral.* **78**, 733-745.

Jensen, M.C., Rota, J.C. & Foord, E.E. (1995): The Gold Quarry mine, Carlin-trend, Eureka County, Nevada. *Mineral. Rec.* **26**, 449-469.

Moore, P.B. (1970): Crystal chemistry of the basic iron phosphates. *Am. Mineral.* **55**, 135-169.

_____ (1984): Crystallochemical aspects of the phosphate minerals. *In* Phosphate Minerals (J.O. Nriagu & P.B. Moore, eds.). Springer-Verlag, New York, N.Y. (155-170).

Nriagu, J.O. (1984): Phosphate minerals: their properties and general modes of occurrence. *In* Phosphate Minerals (J.O. Nriagu & P.B. Moore, eds.). Springer-Verlag, New York, N.Y. (1-136).

VAN DER WESTHUIZEN, W.A., DE BRUIYN, H., BEUKES, G.J. & STRYDOM, D. (1990): Dufrenite in iron-formation on the Kangnas farm, Aggeneys district, Bushmanland, South Africa. *Mineral. Mag.* **54**, 419-424.

VON KNORRING, O., LEHTINEN, M. & SAHAMA, T.G. (1977): Burangaite, a new phosphate mineral from Rwanda. *Bull. Geol. Soc. Finland* **49**, 33-36.

Received June 11, 1997, revised manuscript accepted October 2, 1997.